Dating late Quaternary planktonic foraminifer *Neogloboquadrina pachyderma* from the Arctic Ocean by using amino acid racemization

Darrell S. Kaufman,[1] Leonid Polyak,[2] Ruth Adler,[2] James E.T. Channell,[3] and Chuang Xuan[3]

[1]Department of Geology, Northern Arizona University, Flagstaff AZ 86011, USA.

[2]Byrd Polar Research Center, Ohio State University, 1090 Carmack Road, Columbus, OH 43210, USA.

[3]Department of Geological Sciences, University of Florida, 241 Williamson Hall, P.O. Box 112120, Gainesville, FL 32611, USA.

Abstract. The long-term rate of racemization for amino acids preserved in planktonic foraminifera was determined by using independently dated sediment cores from the Arctic Ocean. The racemization rates for aspartic acid (Asp) and glutamic acid (Glu) in the common taxon, *Neogloboquadrina pachyderma,* were calibrated for the last 150 ka using ^{14}C ages and the emerging Quaternary chronostratigraphy of Arctic Ocean sediments. An analysis of errors indicates realistic age uncertainties of about ± 12% for Asp and ± 17% for Glu. Fifty individual tests are sufficient to analyze multiple subsamples, identify outliers, and derive robust sample mean values. The new age equation can be applied to verify and refine age models for sediment cores elsewhere in the Arctic Ocean, a critical region for understanding the dynamics of global climate change.

1. Introduction

Climate change in the Arctic commands increasing attention as unprecedented shrinkage of sea ice has surpassed the range of historical observations and is likely heading toward a seasonally ice-free Arctic Ocean [e.g., *Comiso et al.,* 2008]. Foreseeing the consequences of this fundamental shift in the state of the Arctic system requires an understanding of past changes in Arctic climatic and oceanic conditions. Meanwhile, acquisition and interpretation of paleoceanographic data in the Arctic face many difficulties. In addition to logistical challenges, studies of Arctic Ocean sedimentary records are hampered by generally low sedimentation rates, limited biogenic proxies due to low productivity and high dissolution, and non-analogous conditions compared with other, better investigated oceanic regions. As a result, despite recent progress in some areas [*Jakobsson et al.,* 2000; *Spielhagen et al.,* 2004; *O'Regan et al.,* 2008], no regional stratigraphic standard for central Arctic Ocean sediments has been developed, and many aspects of their age interpretation are questionable [e.g., *Backman et al.,* 2004; *Sellen et al.,* 2008]. A reliable age model is necessary to place the paleoenvironmental history of the Arctic into a global context, and this requires the advent of new chronostratigraphic approaches.

Considerable advances in the development of age models for Quaternary sediment from the Arctic Ocean have been made since the new stratigraphic paradigm was introduced for cores from the Lomonosov Ridge [*Jakobsson et al.,* 2000], and has been expanded across the central Arctic Ocean [*Backman et al.,* 2004; *Spielhagen et al.,* 2004]. The new approach recognized the complexities of paleomagnetic records, which had been the staple of Arctic Ocean stratigraphy, and used a more realistic assessment of sedimentation rates and placement of paleoclimatic events than in earlier studies [e.g., *Clark et al.,* 1980; *Phillips and Grantz,* 1997]. Recently this new age model has been shown to be consistent with longer-term Cenozoic stratigraphy

developed for the first deep-drilling record from the central Arctic [*O'Regan et al., 2008*]. Nevertheless, many aspects of age assignment within this general stratigraphic framework remain unclear and cannot be resolved by methods that have been applied to date [*O'Regan et al., 2008; Cronin et al., 2008*]. Even more problems arise with stratigraphies from other areas of the central Arctic Ocean [e.g., *Sellen et al., 2008*]. In this paper we advance the use of amino acid racemization in planktonic foraminifers as applied to upper Quaternary sediments from the Arctic Ocean.

The extent of amino acid racemization (AAR) in fossil foraminifera has been used previously to estimate the ages of Quaternary marine sediment (*Kaufman* [2006] reviews previous AAR studies on foraminifera). Deep-marine settings are ideal for amino acid geochronology because of the long-term thermal and geochemical stability of the depositional environment. Foraminifera inhabit most of the world's ocean and they contain high concentrations of amino acids that are well retained by their carbonate test. Sample-size requirements for AAR analysis of foraminifera using reverse-phase chromatography (RPC) are in the sub-milligram range. Preparing samples composed of a small number of tests is less time-consuming than picking larger samples such as for ^{14}C dating or for AAR analysis by the chromatographic techniques used previously, and it can improve the accuracy of the results because the best-preserved individuals can be selected, and because collections of microfossils commonly include a few individuals whose extent of racemization values fall well outside the mean of the others. These outliers might result from post-depositional reworking, post-collection contamination, or an aberrant diagenetic pathway. Regardless of the cause, by routinely analyzing multiple subsamples from a single stratigraphic level, these tests can be identified objectively and excluded from the data set.

Two general approaches are used to convert the extent of AAR to a numeric time scale: In the first approach, the effects of time and temperature on the extent of racemization are determined in modern shells subjected to high-temperature laboratory experiments [e.g., *Kaufman*, 2006]. This relation, together with a model of racemization kinetics, is used to calculate the age of a sample if its temperature history is known. A more secure approach that does not require assumptions about temperature history is to calibrate the rate of racemization by analyzing securely dated samples of a particular taxon from a region where temperature histories are uniform [e.g., *Hearty et al.,* 2004]. The calibrated reaction rate is then used to date samples of the same taxon of unknown age from the same region.

The two previous attempts to use AAR in the Arctic Ocean [*Sejrup et al.*, 1984; *Macko and Aksu,* 1986] used the calibration approach. Both studies relied on only two independently dated samples from the North Atlantic to calibrate the rate of isoleucine epimerization in the foraminifera, *Neogloboquadrina pachyderma.* Because the temperature of bottom water in the North Atlantic is about 4°C higher than in the Arctic Ocean, assumptions were needed to adjust the reaction rate for the Arctic Ocean. Both studies also relied on only a single sample from each stratigraphic level; we find that replication is important for recognizing outliers. Furthermore, both studies were based on isoleucine, which reacts more slowly and therefore has lower temporal resolution than the amino acids that we use in this study. Because of these shortcomings, results of the previous AAR studies in the Arctic Ocean were difficult to interpret conclusively, and during the last 20 years, the approach was not developed further for use in the Arctic Ocean.

In this study, we take advantage of recent developments in the chronostratigraphic framework of Arctic Ocean sediments to calibrate the rate of racemization using control samples

from within the Arctic Ocean itself. We focus on aspartic acid, which affords enhanced age resolution where ambient temperature is low [*Goodfriend et al.,* 1996]. We use these data to develop an AAR age equation for late Quaternary *Neogloboquadrina pachyderma* from the Arctic Ocean, which is applicable to samples as old as 150 ka.

2. Material and Methods

Samples for this study are from three long (piston) sediment cores from three major submarine ridges extending into the central Arctic Ocean: Lomonosov, Mendeleev, and Northwind ridges, plus two multicore samples from the Mendeleev Ridge (Table 1; Figs. 1, 2). Cores HLY0503-8JPC, -10MC and -11MC were collected on the 2005 Healy-Oden TransArctic Expedition (HOTRAX) [*Darby et al.,* 2005]; the data in this paper from these HOTRAX cores have not been presented previously. Litholostratigraphic, paleomagnetic, and microfaunal data from core 88AR-P5 have been published by *Poore et al.* [1993, 1994]; core 96/12-1PC was studied by *Jakobsson et al.* [2000, 2001] and used for correlation by *O'Regan et al.* [2008] as part of the development of the new stratigraphic model for the central Arctic Ocean.

U-channel samples from core HLY0503-8JPC were taken for paleomagnetic analysis. Natural remanent magnetization (NRM) was measured at 1 cm spacing after demagnetization at 14 steps in the 10-100 mT peak field range. Component magnetizations were determined using the standard 3-D least squares method (*Kirschvink*, 1980). The demagnetization range used for calculation of the component directions was non-uniform downcore, and depended on demagnetization behavior of each measurement position, but was usually in the 30-80 mT interval. Maximum angular deviation (MAD) values, associated with the characteristic magnetization components are generally less than 10° for the upper ~420 cm of the core,

indicating that the components are well defined, and then vary widely in the 5°-30° range below that level, indicating that the definition of the characteristic component is highly variable. The onset of negative inclinations at ~420 cm bsf (cm below seafloor) is, however, well defined (Fig. 2), although the control on its position (lithological vs. geomagnetic) has yet to be determined.

Samples for foraminifera and other analyses from core HLY0503-8JPC were taken continuously at 1 cm intervals to 500 cm bsf, freeze dried, washed, and separated by several size fractions. Foraminifers were counted in the >150 μm fraction and picked for AAR analysis from relative abundance peaks throughout the washed portion of the core and, concurrently, for ^{14}C determinations from its upper part. Samples for ^{14}C analyses contained 5 to 8 mg of planktonic foraminifers; no pretreatment was applied.

The rate of amino acid racemization is taxon-dependent and in this study we focus on mono-specific samples of left-coiled *Neogloboquadrina pachyderma*, the predominant Arctic planktonic foraminifer. Approximately 50 tests of adult (encrusted) *N. pachyderma* were picked from intervals with peak foraminifer abundance. They were cleaned by sonicating repeatedly at 1 minute increments until the bath water was clear, then rinsed three times in deionized water. The tests were immersed in 1 mL of 3% H_2O_2 for 2 hr, rinsed with purified H_2O, then air dried under laminar flow. The best-preserved, most-thoroughly cleaned, whole tests were then picked and divided into subsamples composed of 3 to 10 individuals (average = 8), which were placed in sterilized, conical bottomed micro-reaction vials and dissolved in 7 μL of 6 M HCl, and sealed under N_2. To recover the total hydrolysable amino acid population while minimizing the induced racemization, the solutions were hydrolysed at 110°C for 6 hr. Subsamples were evaporated to dryness, rehydrated in 4 μL of 0.01 M HCl with 10 μM L-*h*Arg, an internal spike used to quantify the abundance of amino acids, and injected onto a high-performance liquid

chromoatograph (HPLC).

The chromatographic instrumentation and procedure used to separate amino acid enantiomers is presented by *Kaufman and Manley* [1998], with modifications for individual microfossils described by *Kaufman* [2000, 2003]. Briefly, the analytical method employed pre-column derivatization with *o*-phthaldialdehyde (OPA) together with the chiral thiol, N-isobutyryl-L-cysteine (IBLC), to yield fluorescent diastereomeric derivatives of chiral primary amino acids. The derivatization was performed on-line prior to each injection using the auto-injector of an integrated Agilent 1100 or 1200 HPLC. Separation was by a reverse-phase column packed with a C_{18} stationary phase (Hypersil BDS, 5 µm) using a linear gradient of aqueous sodium acetate, methanol and acetonitrile. Detection was by fluorescence.

The extent of AAR was measured by the ratio of D- to L-enantiomers. The average analytical uncertainty (internal reproducibility) measured by the coefficient of variation for multiple injections of laboratory standards is typically between 2 and 5% for the D/L values of most of the amino acids. Both intra- and inter-laboratory comparative (ILC) samples [*Wehmiller*, 1984] were analyzed routinely to monitor machine performance. For this study, we focused on aspartic acid (Asp) and glutamic acid (Glu), two amino acids that are among the most abundant in foraminifera protein, and are the best resolved chromatographically. More accurately, the Asp and Glu may include a small component of asparagine and glutamine, respectively, which were converted to Asp and Glu during laboratory hydrolysis. Asp and Glu elute during the first 30 min of the sample run, and span most of the range of racemization rates. Serine (Ser) also elutes during this interval and is useful index of contamination, rather than for geochronology. The procedural blank is dominated by Ser, and the blank accounts for an average of 3% and 6% of L-Asp and L-Glu, respectively. The influence of the blank is insignificant at low D/L values, but

increases in older samples as the concentration of indigenous amino acids decrease. No attempt was made to adjust D/L values for the blank.

3. Existing Stratigraphic Context of AAR Samples

3.1. Sediment Core Correlations

The stratigraphy of the cores in this study was tied to the age model developed for the central Lomonosov Ridge [*Jakobsson et al.,* 2000, 2001; *O'Regan et al.,* 2008]. For correlation we use lithological characteristics, foraminiferal abundances, NRM inclination, and benthic foraminiferal events (Fig. 2). Together with new ^{14}C data, this stratigraphy enables the ages of each AAR sample to be estimated independently.

Quaternary sediments in the central Arctic Ocean are generally composed of gray to yellow-brown, nearly abiotic mud alternating with brown, faunal-rich beds interpreted to represent a succession of glaciations and interglacial/ interstadial periods, respectively [*Darby et al.,* 2006 and references therein; *O'Regan et al.*, 2008; *Cronin et al.*, 2008]. This cyclic sedimentation pattern provides the basic framework for stratigraphic correlations across the Arctic Ocean; however, it cannot be used as the sole basis for correlation because of varying sedimentation rates and possible spatial differences in sedimentary environments and preservation of paleontological material. Some additional lithologic features provide more detailed correlation, notably layers of detrital carbonate that were delivered by icebergs from the Canadian Arctic Archipelago during major collapses or surges of the Laurentide ice sheet and dispersed by the Beaufort Gyre [*Bischof and Darby,* 1997; *Phillips and Grantz,* 2001]; however, these features do not occur in the Eurasia Basin and most of the Lomonosov Ridge including core 96/12-1PC.

Paleomagnetic properties, particularly inclination records have been commonly used for stratigraphic correlations of Arctic Ocean sediment [e.g., *Steuerwald et al.*, 1968; *Clark et al.*, 1980; *Backman et al.*, 2004; *Spielhagen et al.*, 2004]. The paleomagnetic inclination of sediment from the central Arctic probably records not only variations in paleomagnetic field, but also changes in rock-magnetic composition, and therefore cannot be used as a simple chronostratigraphic tool [*Jakobsson et al.*, 2000; *O'Regan et al.*, 2008]. Nevertheless, inclination records exhibit an apparently consistent pattern in various regions of the Arctic Ocean and therefore provide an independent means of correlation, regardless of their genesis [e.g., *Spielhagen et al.*, 2004; *Sellen et al.*, 2008]. In particular, the prominent change from predominantly high inclination values to strongly variable including negative values (solid tie line in Fig. 2), previously interpreted as the Bruhnes-Matuyama polarity boundary, is now used as a chronostratigraphic marker in the middle of marine isotope stage (MIS) 7, based on the current age model [*Jakobsson et al.*, 2000; *O'Regan et al.,* 2008].

The abundance of planktonic foraminifers shows a spiky distribution with maxima in brown units in the upper part of all three cores (Fig. 2). The absolute abundance of tests differs between the cores, probably due to different degrees of carbonate dissolution, but relative downcore changes have a consistent pattern. Below the stratigraphic level assigned to MIS 7, sediments throughout the Arctic Ocean are mostly barren of calcareous fossils; instead, arenaceous foraminifers become common and their abundance varies with glacial-interglacial cycles [*Jakobsson et al.*, 2001; *Backman et al.*, 2004; *Cronin et al.*, 2008]. This level probably marks the general weakening of carbonate dissolution in the deep Arctic Ocean and can be used as an aditional stratigraphic marker.

The chronostratigraphic framework is further constructed using benthic foraminiferal

assemblages that contain unique components – species that are otherwise absent or sparse in other stratigraphic levels. These foraminiferal events have been described for the cores in this study or from adjacent sites [*Poore et al.,* 1994; *Ishman et al.*, 1996; *Jakobsson et al.*, 2001; *Polyak et al.*, 2004]. Among the most prominent events are the abundance maximum of *Bulimina aculeata,* and the occurrence of *Epistominella exigua* (dashed tie lines in Fig. 2). Neither species lives in the central Arctic Ocean today, evidently not adapted to perennial ice conditions. Regardless of what caused their previous expansions into the high Arctic, such species occurrences are valuable stratigraphic markers. These events correspond with MIS 5a and 5e, potentially the warmest, low-ice intervals of the late Quaternary [*Nørgaard-Pedersen et al.*, 2007].

3.2. Age Control

Eleven samples from the upper 63 cm in HLY0503-8JPC and two additional samples from the northern part of the Mendeleev Ridge (HLY0503-MC10 and -MC11) were dated by AMS ^{14}C for this study (Table 2). An additional ^{14}C age for the top sample in core 88AR-P5 was taken from *Poore et al.* [1994]. Because of uncertainties in the reservoir age in the Arctic Ocean, we have not applied a ΔR to age calibration. Adult *N. pachyderma* in the central Arctic Ocean live mostly in the lower halocline [e.g., *Volkmann,* 2000], which is ventilated rapidly, on the order of 10 yr in modern conditions [*Ekwurzel et al.*, 2001]. The influence of riverine inputs from Siberia on ΔR in this water cannot be estimated conclusively; limited data from the Laptev Sea indicate a ΔR value between −100 and 460 yr [*Bauch et al.*, 2001]. In the past, especially during discharges of large volumes of glacial meltwater, reservoir ages may have been greater, so the ^{14}C ages from these periods should be considered maximum ages. As a guideline, we assume that

intervals containing planktonic foraminifera with high values of $\delta^{13}C$, which faithfully correspond to brown units [*Poore et al.*, 1999; *Polyak et al.*, 2004], were associated with high ventilation rates. Other complications in the ^{14}C chronology might stem from bioturbation of overall thin interglacial/interstadial units and the input of old carbonaceous water during the discharges of Laurentide detrital carbonates. The latter possibility has not yet been investigated, but potentially can bias ^{14}C ages in the Amerasia Basin, especially at sites proximal to the Canadian Arctic. Generally, ^{14}C ages in HLY0503-8JPC show an orderly succession, consistent with ages obtained earlier from the Mendeleev Ridge [*Darby et al.*, 1997; *Polyak et al.*, 2004]. Some pre-Holocene ages, however, are older than expected by a few thousand years, possibly reflecting the influence of old carbonaceous water, and one sample appears too young, possibly resulting from bioturbation.

Below the range of ^{14}C dating, sample ages are based on correlation with global MIS record [the orbitally-tuned, staked oxygen-isotope record typically referred to as SPECMAP, *Martinson et al.*, 1987], as first proposed by *Jakobsson et al.* [2000] for core 96/12-1PC, and further developed on correlative cores, including the IODP core from the Lomonosov Ridge [*Spielhagen et al.*, 2004; *O'Regan et al.*, 2008]. The general validity of this age model for the upper Quaternary is corroborated for example by correlation of units containing abundant coarse ice-rafted debris and related meltwater indicators with major ice advances along the margins of the Arctic Ocean [*Spielhagen et al.*, 2004], and the presence of subpolar foraminifers at levels corresponding to the warmest intervals, MIS 5a and 5e [*Nørgaard-Pedersen et al.*, 2007]. The resulting age assignment of samples is coarse, but it provides an internally consistent stratigraphic framework suitable for a first-order calibration of the rate of AAR. It is reasonable to assume that the age error for our calibration samples is typically less than one-half of the

duration of a marine isotope substage, that is, within ± 10%.

4. AAR Results

A total of 47 samples of *N. pachyderma* were analyzed for this study. Each sample comprised 2 to 9 subsamples (average = 5; total = 249) (see Supplemental Appendix, "Extent of amino acid racemization (D/L) for aspartic acid (Asp), glutamic acid (Glu), and serine (Ser) in *Neogloboquadrina pachyderma* from Arctic Ocean cores"). Some subsamples yielded D/L values that were clear outliers compared with others from the same sample (Fig. 3). The cause of the variation is not clear. Outliers might reflect reworking of individual tests and are useful for understanding time averaging and age structure in the fossil record [e.g., *Kosnik and Kaufman*, 2008]. In this study, the goal is to derive a robust estimate of the central tendency of D/L values, and a reasonable estimate of the uncertainty of the mean D/L of a sample. Excluding outliers is therefore justified, provided that an objective and reproducible screening procedure is employed. We used a three-step screening procedure to systematically identify outliers. Rejected results are listed and the specific screening criterion applied is tracked for each subsample (Supplemental Appendix). The criteria are: (1) The concentration of serine (Ser) was used to identify subsamples with aberrantly high levels of this labile amino acid, presumably resulting from contamination by modern amino acids. Subsamples with L-Ser/L-Asp > 0.8 were rejected ($n =$ 30). (2) Next, the well-defined covariance between the D/L values of Glu and Asp was used to identify subsamples whose extent of racemization in this pair of amino acids deviated from the trend of other analyses in this study ($n = 3$). (3) Subsamples with D/L Asp or Glu that fell beyond ± 2σ of the mean of the rest of the group, after screening by the two above criteria, were rejected, and this procedure was not iterated ($n = 8$). In all, 41 out of 249 subsamples were

12

rejected, or 16% of the data.

The rejected subsamples had D/L values that were generally lower than the other subsamples. Overall, the sample mean D/L values increased by an average of 0.030 for Asp and 0.012 for Glu, following screening for the 29 samples with one or more rejected subsamples. This is consistent with high L-Ser content of most of the rejected subsamples, which indicates contamination by modern amino acids. Overall, however, the abundance of Asp and Glu was not notably higher for rejected subsamples (Fig. 4), suggesting that a small amount of contamination can significantly impact the D/L values. Although screening had little effect on the mean D/L values and downcore trends, it significantly decreased the intra-sample variability. Following data screening, the intra-sample variability (CV) decreased from 21% to 5% for D/L Asp, and from 29% to 10% for D/L Glu. Overall, following screening, standard errors (σ_x) of mean D/L values average 2.4% for Asp and 5.0% for Glu, which can largely be attributed to analytical precision.

The abundance of amino acids decreases with increasing extent of racemization (Fig. 4), as expected because amino acids degrade or are leached from the tests with time. The amino acid abundance values depend on the mass of the individual foraminifera tests, which varies among samples. On average, the mass of a single *Neogloboquadrina pachyderma* test analyzed in this study is between 8 and 10 µg. On this basis, the concentration of amino acids per mass of carbonate in *N. pachyderma* is similar to that of the larger planktonic foraminifera *Pulleniatina*, which as been analyzed extensively in sediment cores [*Hearty et al.*, 2004] and laboratory heating experiments [*Kaufman*, 2006]. The amino acid content of *N. pachyderma* decreases more rapidly with increasing racemization extent than that of *Pulleniatina*, however, indicating a higher rate of amino acid attrition for *N. pachyderma.*

5. Discussion

5.1. AAR Correlations Among Cores

D/L values for both Asp and Glu increase regularly with depth down to about 2 m in all three long cores (Fig. 5). The values then level off below this depth, corresponding to an age of about 150 ka. Some decrease in the rate of racemization with increasing age is expected as this reversible reaction approaches equilibrium. In the case of the *N. pachyderma* from the Arctic Ocean, however, it appears that D/L values plateau at around 0.4 in Asp and 0.2 for Glu. This plateau is unlikely to have been caused by a shift from overall lower temperature prior to 150 ka to higher temperature since then, because site temperatures are currently near the freezing point. The D/L values in the two amino acids covary strongly in subsamples below this level, and none of the subsamples contain excessive Ser content (Fig. 3), suggesting that the extent of racemization follows the expected diagenetic pathway. If so, then some of the samples below 2 m could be younger than we have assumed. On the other hand, when heated in the laboratory, planktonic foraminifera of the genus *Pulleniatina* show a sharp decrease in the rate of racemization at around the same D/L values, although D/L values continue to increase with heating time (Fig. 4 in [*Kaufman*, 2006]). Determining whether the D/L values plateau or whether they continue to increase with age and depth will require further analyses.

The two unique benthic foraminifera events and the shift in paleomagnetic characteristics (Fig. 2) provide chronostratigraphic markers to compare D/L values among the three long cores (Fig. 3). The D/L values for both Asp and Glu overlap within $\pm 1\sigma$ (or $\pm 2\sigma_x$) for the three samples from each of the marker horizons. The D/L values vary by 2 to 6% for Asp and 5 to 9% for Glu. Most of the difference in D/L values among correlative horizons in different cores can

be ascribed to analytical errors and intra-sample variability, mutually supporting the integrity of the stratigraphic correlations and the AAR results.

5.2. AAR Age Equation

The chronostratigraphic ages and the ^{14}C ages from all five cores were aggregated to develop a calibrated age equation that relates the extent of racemization in *N. pachyderma* to sample age (Table 3). Following the procedure discussed by *Kosnik et al.* [2008], we modeled the rate of racemization using a simple power transformation and chose the exponent that best linearized the trend in D/L versus sample age based on least-squares regression forced through the origin (Fig. 6). Samples older than 150 ka could not be modeled using a power transformation and were excluded from the age model. Least-squares linear regressions based on the remaining 38 samples yield the age equations for *N. pachyderma* from the Arctic Ocean for up to 150 ka. The age equation for Asp is:

$$t = 920(D/L)^{2.3} \qquad (r^2 = 0.884; P < 0.001) \qquad (1)$$

and for Glu

$$t = 1462(D/L)^{1.6} \qquad (r^2 = 0.774; P < 0.001) \qquad (2)$$

where t = age in ka.

The accuracy of ages derived from this procedure depends on an array of variables. A Monte Carlo simulation was used to quantify the overall age uncertainty in the AAR age model, and to assess its sensitivity to the input variables. The results of this simulation show that the accuracy of the AAR ages is primarily and linearly related to the uncertainty in the independent ages that are used to calibrate the rate of racemization. For each ± 10% change in the uncertainty in the calibration ages, the corresponding change in the accuracy of AAR ages is about ± 1.3%,

15

assuming that the uncertainty in the D/L value (intra-sample variability) is characterized by $\pm$ $1\sigma_x$. Using $\pm 2\sigma_x$ to characterize the intra-sample variability reduces the *sensitivity* of the AAR age accuracy to changes in the uncertainty associated with the calibration ages. At $\pm 2\sigma_x$ the intra-sample variability is the primary uncertainty in the overall age estimate, and the resulting accuracy of the AAR ages is about $\pm$ 12% for Asp and about $\pm$ 17% for Glu, regardless of whether the uncertainty in the calibration ages is 10% or 30%, for instance.

Quantifying the uncertainty in the independent ages used to calibrate the rate of racemization is difficult. Instead, we rely on conventional regression statistics to estimate the uncertainty in the rate of racemization as derived from the combined data set ($n = 38$). The standard error of the slope of the least-squares regression (rate of racemization) is $\pm$ 54 ka $(D/L)^{-2.3}$ for Asp, and $\pm$ 136 ka $(D/L)^{-1.6}$ for Glu. Combining this error in the slope with the typical $\pm$ $2\sigma_x$ in mean D/L values determined from our samples (Asp = $\pm$ 4.8%; Glu = $\pm$ 10.0%) yields an overall realistic age error of about $\pm$ 12% for Asp and $\pm$ 17% for Glu for samples within the age range of the calibration equations (up to about 150 ka). This compares with standard error of the sample, based on the residuals, of 14 ka for Asp and 19 ka for Glu.

Both the regression fit and the intra-sample variability are better for Asp than for Glu, implying that Asp is a superior chronometer for these samples. For samples with D/L values higher than about 0.5, however, the rate of racemization for Asp decreases beyond that for Glu, suggesting that Glu might out-perform Asp for older samples. Regardless, tracking D/L values for both amino acids is important because, although the rate of racemization in Asp and Glu are affected by the same systematic errors and are therefore not strictly independent, samples that yield similar ages for the two amino acids are viewed with greater confidence. *Kosnik and Kaufman* [2008] suggest that samples that yield ages for Asp and Glu that differ by more than

20% should be considered suspect. Otherwise, the ages can be averaged to generate a single age.

These uncertainties are less than those estimated for the planktonic foraminifer, *Pulleniatina*, which are based on racemization kinetics analyzed in the laboratory (the first approach described above), with an assumed temperature uncertainty of ± 0.5°C [*Kaufman*, 2006]. The enhanced age resolution for *N. pachyderma* can in part be attributed to its relatively high rate of racemization, which is about twice as high for samples from the Arctic Ocean than for *Pulleniatina* from the Queensland Trough, Australia [*Hearty et al.*, 2004] (Fig. 6), despite bottom water temperatures that are a least a few degrees lower in the deep Arctic Ocean (–1° to 0ºC in the Arctic Ocean compared with 2°C for Queensland Trough). The higher rate of racemization in *N. pachyderma* seems inconsistent with its higher rate of amino acid attrition (discussed above) and suggests that, if amino acids are lost to leaching, they are not preferentially leached from the more highly racemized free amino acid fraction. We suggest that the proportion of amino acids within the intra-crystalline fraction, which is dominated by free amino acids in carbonate fossils [*Penkman et al.*, 2008] increases at a higher rate in *N. pachyderma* than in *Pulleniatina*, but this hypothesis awaits testing by analyzing the different amino acid fractions.

6. Conclusions and Implications

AAR values (D/L of aspartic acid and glutamic acid) analyzed in planktonic foraminifer *Neogloboquadrina pachyderma* show a consistent pattern of downcore trends in three sediment cores from the central Arctic Ocean separated by hundreds of kilometers, which confirms the applicability of AAR geochronology to Arctic Ocean stratigraphy. Calibration of the rate of racemization by independent age assignments (^{14}C ages and correlations with the global MIS

record using the Lomonosov Ridge stratigraphy as reference) shows a convincing correlation between D/L values and age, at least for the late Quaternary. These results indicate that AAR, which can be measured on small numbers of foraminifers, provides a useful tool for stratigraphic correlation and late Quaternary geochronology in the Arctic Ocean. To confidently correlate stratigraphic sequences with reference records, such as in this paper, requires multiple stratigraphic techniques at relatively high sample resolution, which may not be feasible for many sites. The AAR approach offers a fast and cost-efficient method for checking the age of target intervals identified by lithostratigraphic correlation across the Arctic Ocean, even in low-resolution cores. As a stratigraphic tool, the technique is unencumbered by uncertainties related to the ^{14}C reservoir age, and is applicable beyond the range of ^{14}C dating. Sediment cores from the Nordic seas might provide suitable material for refining and extending the AAR calibration for the Arctic Ocean because bottom water temperatures in the Nordic seas are similar to those in the Arctic Ocean (near -1°C), and the stratigraphy for the last 500 ka is well developed and correlated with North Atlantic records (e.g., *Bauch and Erlenkeuser,* 2003; *Helmke and Bauch,* 2003).

The late Quaternary time interval is especially important for paleoclimatic studies as it encompasses the last interglacial, potentially the closest analog for the projected future, low-ice or even seasonally ice-free state of the Arctic [*Otto-Bliesner et al.*, 2006]. To date, the last interglacial in the Arctic has been characterized based mostly on sites along the Arctic periphery [CAPE, 2006], and without a reliable stratigraphic framework for the identification of the last interglacial in sedimentary records from the central Arctic Ocean. The AAR geochronology developed here offers a new possibility for resolving this problem with a reasonable accuracy for sediment cores that contain at least small numbers of planktonic foraminifera.

References

Backman, J., M. Jakobsson, R., Løvlie, L. Polyak, and L. A. Febo (2004), Is the central Arctic Ocean a sediment starved basin? *Quat. Sci. Rev.*, 23, 1435-1454.

Bauch, H.A., and H. Erlenkeuser (2003), Interpreting glacial-interglacial changes in ice volume and climate from subarctic deep water foraminiferal $\delta^{18}O$, In: *Earth's Climate and Orbital Eccentricity: The Marine Isotope Stage 11 Question, Geophysical Monograph Series*, 137, 87-102.

Bauch, H.A., Mueller-Lupp, T., Taldenkova, E., Spielhagen, R.F., Kassens, H., Grootes, P.M., Thiede, J., Heinemeier, J., and Petryashov, V.V. (2001), Chronology of the Holocene transgression at the North Siberian margin, *Global Planet. Change*, 31, 125–139.

Bischof, J. A. and D. A. Darby (1997), Mid to late Pleistocene ice drift in the western Arctic Ocean: evidence for a different circulation in the past, *Science*, 277, 74-78.

CAPE-Last Interglacial Project Members (2006), Last interglacial Arctic warmth confirms polar amplification of climate change, *Quat. Sci. Rev.*, 25, 1383-1400.

Clark, D.L., Whitman, R.R., Morgan, K.A., and Mackey, S.D., 1980. Stratigraphy and glacial-marine sediments of the Amerasian Basin, central Arctic Ocean. Geologial Society of America Special Paper 181, 57p.

Comiso, J. C., et al. (2008), Accelerated decline in the Arctic sea ice cover, *Geophy. Res. Lett.*, 35, doi:10.1029/2007GL031972.

Cronin, T. M., S. Smith, F. Eynaud, M. O Regan, and J. King (2008), Quaternary paleoceanography of the central Arctic based on IODP ACEX 302 foraminiferal assemblages, *Paleoceanography*, in press.

Darby, D. A., J. F. Bischof, and G. A. Jones (1997), Radiocarbon chronology of depositional regimes in the western Arctic Ocean, *Deep-Sea Res.*, 44, 1745-1757.

Darby, D., M. Jakobsson, and L. Polyak (2005), Icebreaker expedition collects key Arctic seafloor and ice data, *EOS Trans. AGU,* 86(52), 549-556.

Darby, D. A., L. Polyak, and H. Bauch (2006), Past glacial and interglacial conditions in the Arctic Ocean and marginal seas - a review, in *Structure and Function of Contemporary Food Webs on Arctic Shelves: A Pan-Arctic Comparison,* edited by P. Wassman, *Prog. Oceanography*, 71, 129-144.

Ekwurzel, B., P. Schlosser, R. A. Mortlock, R. G. Fairbanks, and J. H. Swift (2001), River runoff, sea ice meltwater and Pacific water distribution and mean residence times in the Arctic Ocean, *J. Geophys. Res.*, 106, 9075-9092.

Fairbanks, R. G., Mortlock, R. A., Chiu, T.-C., Cao, L., Kaplan, A., Guilderson, T. P., Fairbanks, T. W., and Bloom, A. L. (2005). Marine radiocarbon calibration curve spanning 0 to 50,000 years B.P. based on paired ^{230}Th/^{234}U/^{238}U and ^{14}C dates on pristine corals, *Quatern. Sci. Rev.*, 24, 1781-1796.

Goodfriend, G. A., J. Brigham-Grette, and G. H. Miller (1996), Enhanced age resolution of the marine Quaternary record in the Arctic using aspartic acid racemization dating of bivalve shells, *Quat. Res.*, 45, 176-187.

Hearty, P. J., M. J. O'Leary, D. S. Kaufman, M. Page, and J. Bright (2004), Amino acid geochronology of individual foraminifer (*Pulleniatina obliquiloculata*) tests, north Queensland margin, Australia: A new approach to correlating and dating Quaternary tropical marine sediment cores, *Paleoceanography*, 19, PA4022, doi:10.1029/2004PA001059.

Helmke, J. P., and H.A. Bauch (2003), Comparison of glacial and interglacial conditions between the polar and subpolar North Atlantic region over the last five climatic cycles, *Paleoceanography*, 18 (2), 1036, doi:10.1029/2002PA000794.

Ishman, S. E., L. V. Polyak, and R. Z. Poore (1996), Expanded record of Quaternary oceanographic change: Amerasian Arctic Ocean, *Geology*, 24, 139-142.

Jakobsson, M., N. Cherkis, J. Woodward, B. Coakley, and R. Macnab (2000), A new grid of Arctic bathymetry: A significant resource for scientists and mapmakers, *EOS Trans. AGU,* 81(9), 89, 93, 96.

Jakobsson, M., R. Løvlie, H. Al-Hanbali, E. Arnold, J. Backman, and M. Mörth (2000), Manganese color cycles in Arctic Ocean sediments constrain Pleistocene chronology, *Geology*, 28, 23-26.

Jakobsson, M., R. Løvlie, E. M. Arnold, J. Backman, L. Polak, J. O. Knutsen, and E. Musatov (2001), Pleistocene stratigraphy and paleoenvironmental variation from Lomonosov Ridge sediments, central Arctic Ocean. *Global Planet. Change*, 31, 1-22.

Kaufman, D. S. (2000), Amino acid racemization in ostracodes, in *Perspectives in Amino Acid and Protein Geochemistry*, edited by G. Goodfriend et al., pp. 145-160, Oxford Univ. Press,

New York.

Kaufman, D. S. (2003), Dating deep-lake sediments by using amino acid racemization in fossil

ostracodes, *Geology*, 31, 1049-1052.

Kaufman, D. S. (2006), Temperature sensitivity of aspartic and glutamic acid racemization in the

foraminifera *Pulleniatina*, *Quat. Geochron.*, 1, 188-207.

Kaufman, D. S., and W. F. Manley (1998), A new procedure for determining enantiomeric (D/L)

amino acid ratios in fossils using reverse phase liquid chromatography. *Quat. Sci. Rev.*, 17,

987-1000.

Kirschvink, J.L., 1980, The least squares lines and plane analysis of paleomagnetic data:

Geophys. J.R. Astr. Soc., 62, 699-718..

Kosnik, M. A., and D. S. Kaufman (2008), Identifying outliers and assessing the accuracy of

amino acid racemization measurements for geochronology: II. Data screening, *Quat.*

Geochron., 3, 328-341.

Kosnik, M. A., D. S. Kaufman, and Q. Hau (2008), Identifying outliers and assessing the

accuracy of amino acid racemization measurements for geochronology: I. Age calibration

curves, *Quat. Geochron.,* 3, 308-327.

Martinson, D. G., N. G. Pisias, J. D. Hays, J. Imbrie, T. C. Moore, and N. J. Shackleton (1987),

Age dating and the orbital theory of the ice ages - development of a high-resolution 0 to

300,000-year chronostratigraphy, *Quat. Res.*, 27, 1-29.

Macko, S. A., and A. E. Aksu (1986), Amino acid epimerization in planktonic foraminfera

suggests slow sedimentation rates for Alpha Ridge, Arctic Ocean, *Nature*, 322, 730-732.

Nørgaard-Pedersen, N., N. Mikkelsen, and Y. Kristoffersen (2007), Arctic Ocean record of last

two glacial-interglacial cycles off North Greenland/Ellesmere Island - Implications for

glacial history, *Marine Geol.*, 244, 93–108.

O'Regan, M., J. King, J. Backman, et al. (2008), Constraints on the Pleistocene chronology of

sediments from the Lomonosov Ridge, *Paleoceanography,* (in press).

Otto-Bliesner, B. L., S. J. Marshall, J. T. Overpeck, G. H. Miller, A. Hu, and C. L. I. members

(2006), Simulating arctic climate warmth and icefield retreat in the last interglaciation,

Science, 311, 1751-1753.

Penkman, K. E. H., D. S. Kaufman, D. Maddy, and M. J. Collins (2008), Closed-system

behaviour of the intra-crystalline fraction of amino acids in mollusk shells, *Quat. Geochron.,*

3, 2-25.

Phillips, R.L., and A. Grantz, 1997, Quaternary history of sea ice and paleoclimate in the

Amerasia basin, Arctic Ocean, as recorded in the cyclical strata of Northwind Ridge. Geol.

Soc. Amer. Bull., 109, 1101-1115.

Phillips, R. L., and A. Grantz (2001), Regional variations in provenance and abundance of ice-

rafted clasts in Arctic Ocean sediments: implications for the configuration of late Quaternary

oceanic and atmospheric circulation in the Arctic, *Marine Geol.*, 172, 91-115.

Polyak, L., W. B. Curry, D. A. Darby, J. Bischof, and T. M. Cronin (2004), Contrasting

glacial/interglacial regimes in the western Arctic Ocean as exemplified by a sedimentary

record from the Mendeleev Ridge, *Palaeogeog., Palaeoclimatol., Palaeoecol.*, 203, 73-93.

Poore, R. Z., R. L. Phillips, and H. J.Rieck (1993), Paloeclimate record for Northwind Ridge,

western Arctic Ocean, *Paleoceanography*, 8, 149-159.

Poore, R. Z., S. E. Ishman, R. L. Phillips, and D. H. McNeil (1994), Quaternary stratigraphy and

paleoceanography of the Canada Basin, western Arctic Ocean, *US Geol. Surv. Bull.*, 2080, 32

pp.

Poore, R. Z., L. Osterman, W. B. Curry, and R. L. Phillips (1999), Late Pleistocene and
Holocene meltwater events in the western Arctic Ocean, *Geology*, 27, 759-762.

Sejrup, H. P., G. H. Miller, J. Brigham-Grette, R. Løvlie, and D. Hopkins (1984), Amino acid
epimerization implies rapid sedimentation rates in Arctic ocean cores, *Nature* 310, 772-775.

Sellen, E., M. Jakobsson, and J. Backman (2008), Sedimentary regimes in Arctic's Amerasian
and Eurasian basins: clues to differences in sedimentation rates, *Global and Planet. Change*
61, 275-284.

Spielhagen, R. F., K. H. Baumann, H Erlenkeuser, N. R. Nowaczyk, N. Norgaard-Pedersen, C.
Vogt, and D. Weiel (2004), Arctic Ocean deep-sea record of northern Eurasian ice sheet
history, *Quat. Sci. Rev.*, 23, 1455–1483.

Steuerwald, B. A., D. L. Clark, and J. A. Andrew (1968), Magnetic stratigraphy and faunal
patterns in Arctic Ocean sediments, *Earth Planet. Sci. Lett.*, 5, 79-85.

Volkmann, R. (2000), Planktic foraminifers in the outer Laptev Sea and the Fram Strait –
modern distribution and ecology, *J. Foraminiferal Res.*, 30, 157-176.

Wehmiller, J. F. (1984), Interlaboratory comparison of amino acid enantiomeric ratios in fossil
Pleistocene mollusks, *Quat. Res.*, 22, 109-120.

Figure Captions

Figure 1. Arctic Ocean with major geographic features and circulation systems, Beaufort Gyre (solid lines) and Transpolar Drift (punctured). Cores 96/12-1PC, HLY0503-8JPC, and 88AR-P5 are shown by stars on the Lomonosov, Mendeleev, and Northwind Ridges (LR, MR, and NR), respectively; multicores are shown by circles. Base map from International Bathymetric Chart of the Arctic Ocean [*Jakobsson et al.*, 2000].

Figure 2. Correlation among sediment cores used in this study, showing the main lithologic features, planktonic foraminiferal abundance (black curves), and paleomagnetic inclination (grey curves) (for cores 96/12-PC and 88AR-P5, see *Jakobsson et al.* [2000, 2001] and *Poore et al.* [1993, 1994], respectively). Note that paleomagnetic measurements are much more sparse in 88AR-P5 than in the other two cores. Solid tie line — natural remanent magnetization (NRM) inclination shift. Ba and Ee (dashed tie lines) — abundance maxima or unique presence events for benthic foraminifers *Bulimina aculeata* and *Epistominella exigua*, respectively. Dotted tie lines – major detrital carbonate layers. Triangles — position of samples analyzed for amino acid racemization. Assignment of marine isotopic stages (MIS) is based on the age model developed for the central Lomonosov Ridge [*Jakobsson et al.*, 2000; *O'Regan et al.*, 2008]. Ages of MIS boundaries [*Martinson et al.*, 1987] are shown in italics.

Figure 3. Extent of racemization (D/L) in aspartic acid (Asp) and glutamic acid (Glu) in individual subsamples of *Neogloboquadrina pachyderma* from the Arctic Ocean. Subsamples rejected based on three screening criteria are indicated. Data listed in Supplemental Appendix.

Figure 4. Amino acid abundance in subsamples of *Neogloboquadrina pachyderma* from the Arctic Ocean. Abundance values are the sum of aspartic acid (Asp), glutamic acid (Glu), and serine (Ser) per individual foraminifer. The mass of each test averages 8-10 μg. The abundance of amino acids decreases with increasing racemization (age) and is similar for accepted and rejected subsamples. Data listed in Supplemental Appendix.

Figure 5. Extent of racemization (D/L) in aspartic acid (Asp) and glutamic acid (Glu) in samples of *Neogloboquadrina pachyderma* plotted according depth in five sediment cores from the Arctic Ocean. Tie lines connect samples from specific stratigraphic events discussed in the text and shown in Fig. 2, including: inclin — paleomagnetic inclination shift; Ba and Ee — *Bulimina aculeata* and *Epistominella exigua* events, respectively; dc — samples adjacent to the upper detrital carbonate layer. Data listed in Table 3.

Figure 6. Rate of racemization in (A) aspartic acid (Asp) and (B) glumatic acid (Glu) in independently dated samples of *Neogloboquadrina pachyderma* from the Arctic Ocean. Least-squares linear regressions are based on samples <150 ka only. Samples shown in grey symbols were not included. Data listed in Table 4. Grey curve — rate of racemization in *Pulleniatna* from the Queensland Trough, Australia [*Hearty et al.*, 2004].

Table 1. Sediment Cores Analyzed for This Study

Core[a]	Vessel and year	Coordinates	Water depth (m)	Region	Source of data used in Fig. 2
HLY0503-8JPC	Healy, 2005	79° 35.6' N 172° 30.1' W	2792	Mendeleev Ridge	This paper
HLY0503-10MC-2	Healy, 2005	81°13.7' N 177°13.0'W	1841	Mendeleev Ridge	This paper
HLY0503-11MC-2	Healy, 2005	83°07.7' N 174°41.6'W	2570	Mendeleev Ridge	This paper
96/12-1PC	Oden, 1996	87° 05.9' N 144° 46.4' E	1003	Lomonosov Ridge	*Jakobsson et al.,* 2000, 2001
88AR-P5	Polar Star, 1988	74° 37.35' N 157° 53.04' W	1089	Northwind Ridge	*Poore et al.,* 1993, 1994

[a]MC — multicores, all other cores — piston cores.

Table 2. Radiocarbon Ages of Planktonic Foraminifers Used to Calibrate Rate of Racemization

Lab ID[a]	HLY0503 core ID	Depth in core (cm)	^{14}C age (yr BP)	1 σ (±)	Calibrated age (yr BP)[b]	1 σ range (±)
AA74470	8JPC	0-1	3981	46	3984	72
AA74471	8JPC	7-8	9314	76	10,151	103
AA74472	8JPC	14-15	8940	63	9608	79
AA74473	8JPC	24-25	9917	50	10,857	127
AA77887	8JPC	32-33	36.250	730	41,118	681
AA74475	8JPC	34-35	32,480	470	37,467	502
AA74476	8JPC	43-44	38,660	980	43,218	863
AA74477	8JPC	48-49	30,950	400	35,926[c]	404
AA74478	8JPC	52-53	>43,300	na	na	na
AA74479	8JPC	56-57	37,820	880	42,493	781
AA74480	8JPC	62-63	40,500	1300	44,816	1149
AA75845	10MC2	10-11	31,760	430	36,731	457
AA75847	11MC2	5-6	26,140	220	30,949	270

[a]All samples were analyzed by AMS at the NSF Radiocarbon Facility, University of Arizona.

[b]Holocene ages are median probability ages based on calibration using CALIB v 5.0.2

(http://calib.qub.ac.uk/calib/); older ages were calibrated using the Fairbanks0107 program

[*Fairbanks et al.*, 2005]. No ΔR was applied.

[c]Age rejected because it is considerably younger than others above and below it.

Table 3. Extent of Racemization (D/L) in Foraminifera from Arctic Ocean Cores

Lab ID (UAL)	Depth (cm)	n^a	ex^a	Aspartic acid D/L	$\pm \sigma_x$	Glutamic acid D/L	$\pm \sigma_x$	Age $(ka)^b$
88AR-P5								
5921	1	5	0	0.098	0.005	0.050	0.005	5.53
5920	55	5	0	0.248	0.004	0.111	0.005	35
5918	89	5	0	0.288	0.006	0.139	0.004	64
5922	125	4	1	0.349	0.012	0.163	0.015	85
5917	180	3	2	0.380	0.011	0.169	0.006	100
5923	191	4	1	0.406	0.004	0.213	0.005	105
5919	233	4	1	0.404	0.004	0.194	0.003	123
5916	318	4	1	0.395	0.011	0.203	0.006	193
5913	365	4	4	0.408	0.007	0.194	0.004	242
96/12-1PC								
5926	0-1.9	4	2	0.154	0.003	0.088	0.001	10
5927	18.3-20.2	3	2	0.267	0.002	0.118	0.006	35
5928	175.8-177.4	6	1	0.313	0.008	0.146	0.011	79
5929	198.4-200	3	2	0.404	0.017	0.194	0.013	85
5930	206.4-208.1	3	1	0.401	0.014	0.207	0.021	100
5931	219-220.5	5	0	0.392	0.008	0.184	0.010	123
5932	257.5-259	4	1	0.440	0.016	0.230	0.018	193
5933	275-276.6	5	0	0.463	0.013	0.248	0.018	242
HLY0503-8JPC								
6134	0-1	4	1	0.080	0.003	0.035	0.000	3.98
6141	7-8	4	0	0.096	0.004	0.034	0.003	10.15
6140	14-15	2	1	0.108	0.002	0.046	0.004	9.61
6135	24-25	3	1	0.110	0.002	0.039	0.001	10.86
6136	32-33	4	0	0.193	0.007	0.086	0.005	41.12
6142	34-35	6	0	0.190	0.006	0.076	0.006	37.47
6137	43-44	5	1	0.221	0.004	0.104	0.006	43.22
6143	48-49	4	1	0.261	0.005	0.109	0.011	40
6138	52-53	6	0	0.278	0.003	0.132	0.004	42
6144	56-57	4	1	0.285	0.010	0.131	0.014	42.49
6139	62-63	6	0	0.295	0.004	0.143	0.004	44.85
6387	73-74	4	1	0.276	0.009	0.101	0.007	48
6388	83-84	4	1	0.283	0.006	0.123	0.004	51
6389	93-94	2	0	0.344	0.007	0.176	0.008	53
6149	105-106	4	0	0.309	0.004	0.154	0.004	56
6390	115-116	4	1	0.361	0.008	0.177	0.008	61
6391	132-133	3	1	0.355	0.005	0.176	0.005	79
6392	145-146	2	0	0.342	0.013	0.145	0.013	90
6393^c	179-180	4	0	0.462	0.006	0.232	0.006	100
6717	180-181	8	1	0.405	0.008	0.197	0.006	100
6394	226-227	3	2	0.402	0.007	0.188	0.006	123
6395	238-239	5	0	0.395	0.007	0.177	0.007	126
6396	246-247	3	2	0.389	0.005	0.168	0.006	129
6775	282-283	6	0	0.411	0.006	0.201	0.010	147
6718	358-359	6	3	0.400	0.010	0.184	0.005	178
6719	404-405	7	2	0.419	0.010	0.204	0.008	193
6720	418-419	8	1	0.429	0.010	0.211	0.009	196
6776	428-429	6	1	0.441	0.012	0.219	0.016	222
HLY0503-11MC-2								
6510	5-6	5	0	0.225	0.018	0.106	0.011	30.95
HLY0503-10MC-2								
6511	10-11	5	0	0.279	0.009	0.137	0.005	36.73

Inter-laboratory comparison samples[d]

ILC-A	na	9	0	0.372	0.002	0.184	0.001	na
ILC-B	na	9	0	0.685	0.002	0.407	0.001	na
ILC-C	na	9	0	0.889	0.008	0.839	0.001	na

[a]n — Number of subsamples included; ex — number excluded in calculation of mean and standard error.

[b]Ages with two decimals — ^{14}C age (Table 2); other ages — estimated based on stratigraphic correlations.

[c]Sample rejected because D/L values are considerably higher than any in the underlying 2 m of core.

[d]ILC samples [*Wehmiller*, 1984] analyzed during the course of this study.
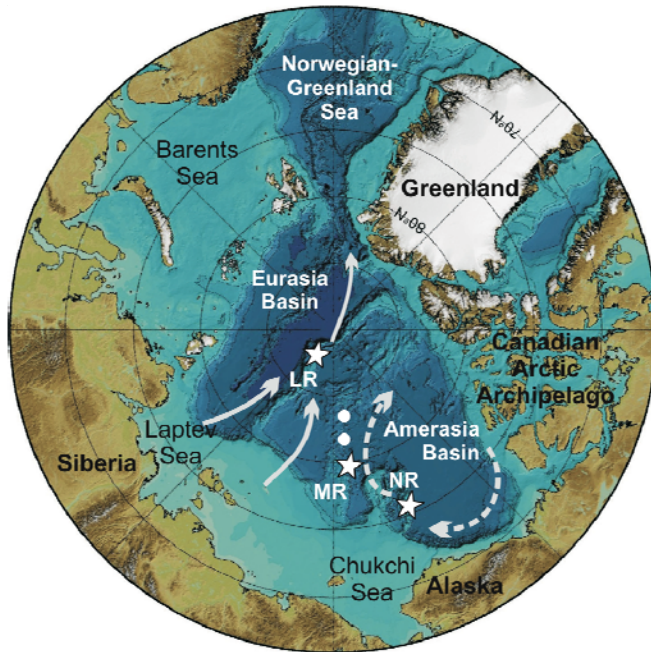
Figure 1
Kaufman et al.
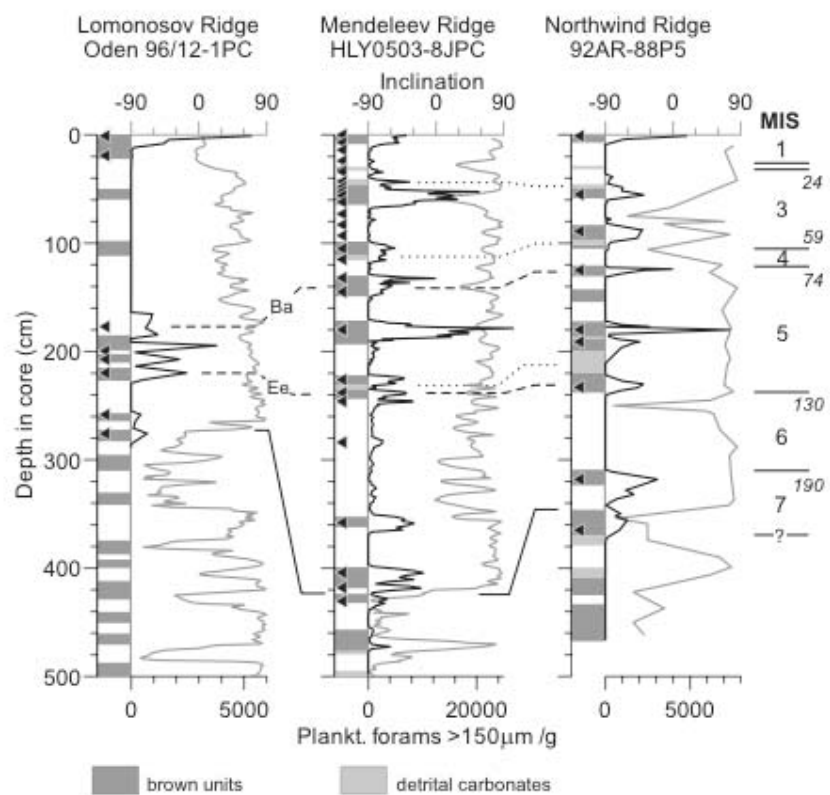
Figure 2
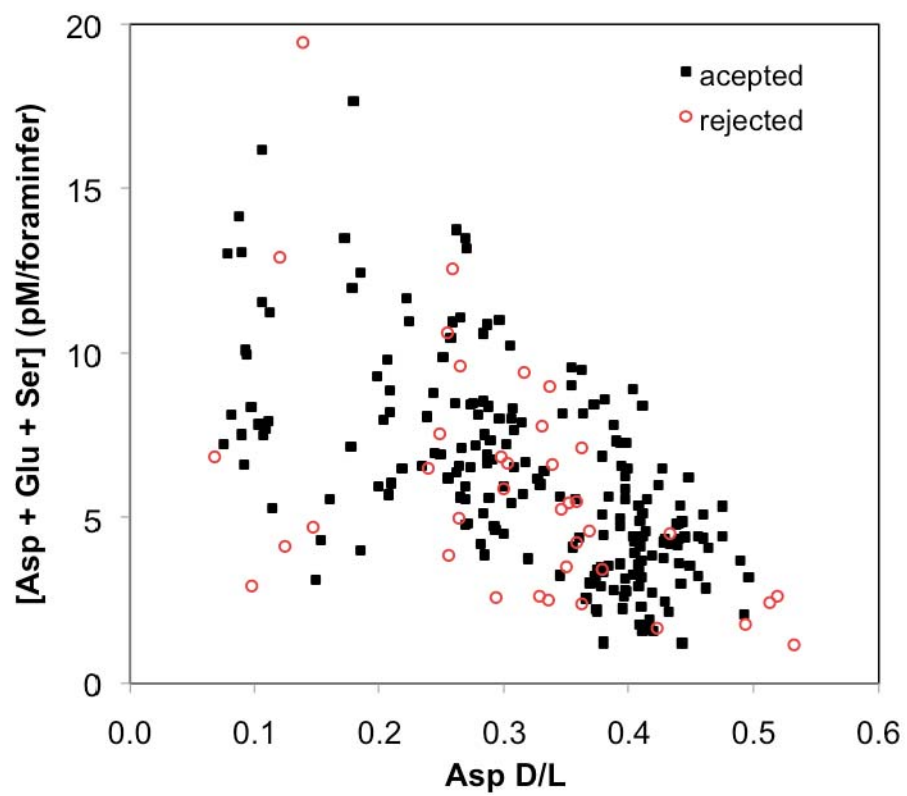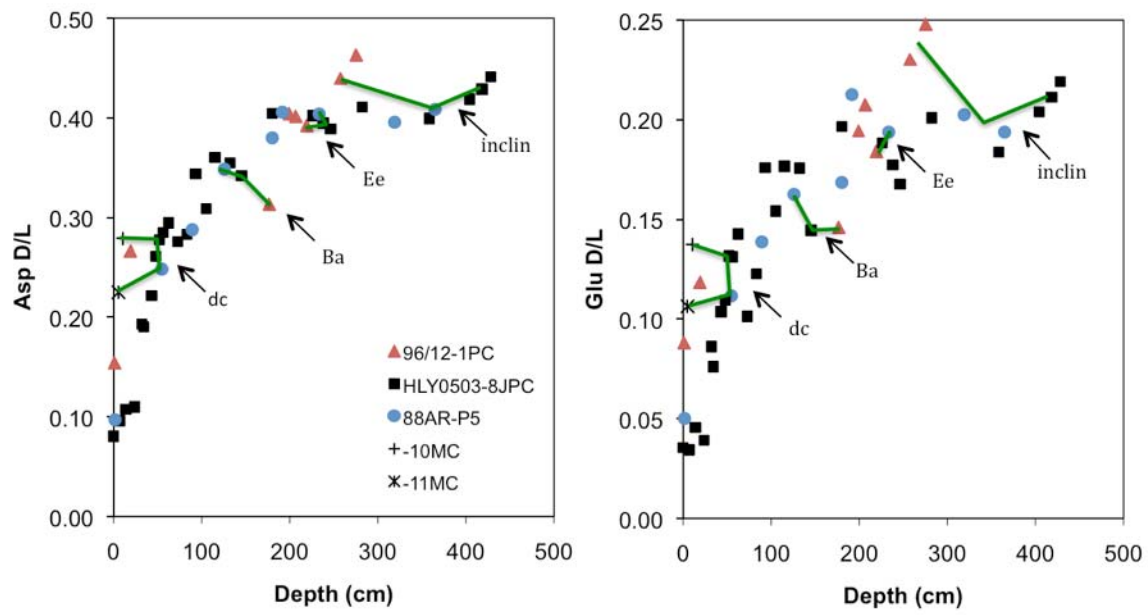
Kaufman et al.
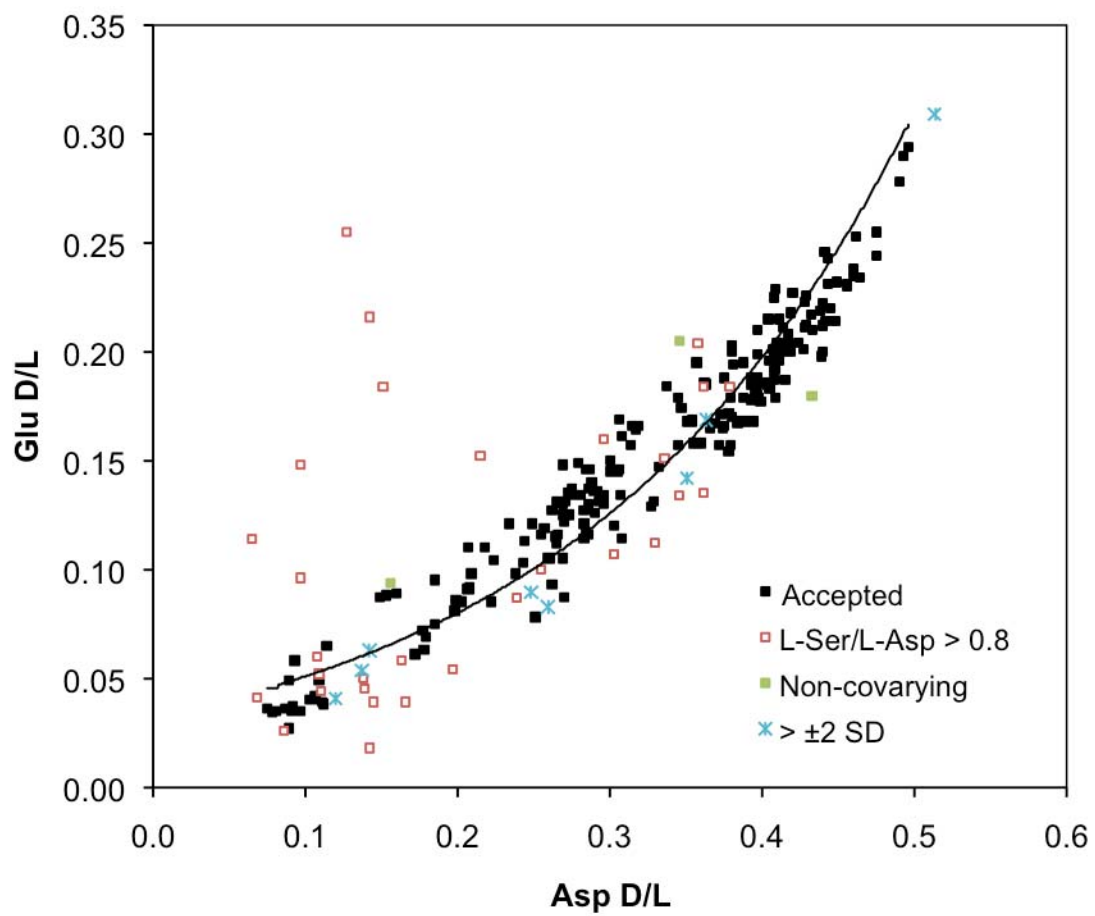
Figure 3
Kaufman et al.

Figure 4
Kaufman et al.
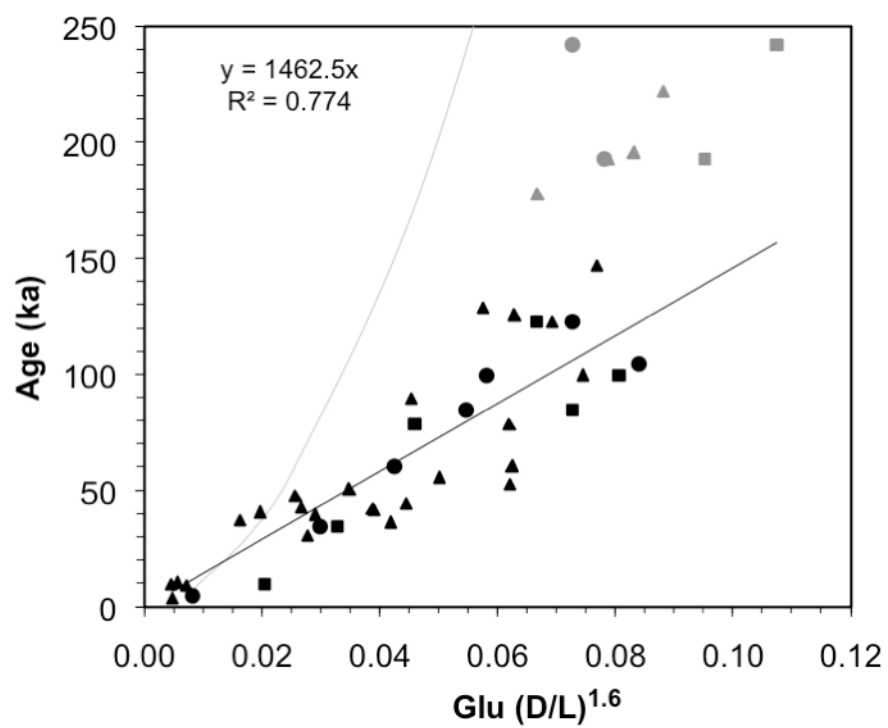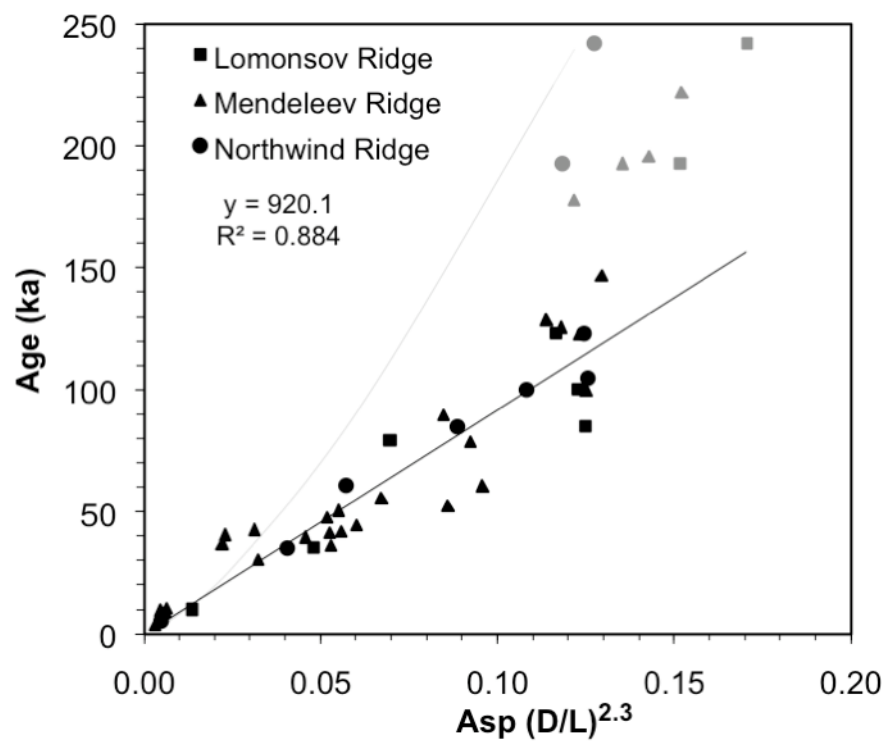
Figure 5
Kaufman et al.

Figure 6
Kaufman et al.